Structural Engineering and Mechanics, Vol.2, No.3 (1994) 227-244
DOI: http://dx.doi.org/10.12989/sem.1994.2.3.227

Numerical simulation of the crack propagation behavior in 3D elastic body

Takeo Taniguchi †, Akihiko Miyaji ‡, Takeshi Suetsugu ‡† & Shohgo Matsunaga ‡‡

Abstract. The purpose of this investigation is to propose a numerical simulation method of the crack propagation behavior in 3-dimensionl elastic body. The simulation method is based on the displacement-type finite element method, and the linear fracture theory is introduced. The results from the proposed method are compared with those from the structural experiments, and the good coincidences between them are shown in this paper. At the same time, 2-dimensional analysis is also done, and the results are compared with those obtained from 3-dimensional analysis and the structural experiments.

Key words: linear fracture theory ; FEM; 3D crack propagation; automatic mesh generation; singular isoparametric element.

1. Introduction

The cracks in a 3-dimensional body become apparent only after they have grown and appear on the surface of the body. But, they are only the result of the crack propagation, and it is difficult for engineers to know how they grow and how they propagate. The main purpose of this investigation is to propose a numerical method for clarifying how cracks in 3-dimensional body grow and propagate.

In the civil, ship-building and mechanical engineering fields, it is required to clarify the mechanism of the crack propagation. For example, at the construction site where old concrete structures need to be removed to be replaced with new ones, engineers have the problem of excising the old portion in the most efficient way possible without damage to the residual structures. And, at the construction site of highways and buildings the cost for the construction is largely governed by the amount of rock which is cut off. In these cases new construction method is required to be developed for saving the cost and also for shortening the construction period, and, for this purpose the mechanism of the crack propagation behavior must be clarified.

The investigation into the field of the fracture mechanics has been done with the result that the linear fracture theory is now almost established. The result is already introduced in the ship-building engineering, aircraft design, steel bridge maintenance, and so on. Most investigations on the application of the linear fracture theory treat 2-dimensional problems,

† Eng. Science Dept., Okayama Univ., Okayama, Japan
‡ Japan Development & Construction Co. Ltd., Minatoku, Tokyo, Japan
‡† Ishikawajima-Harima Heavy Industry Co., Kure-shi, Horoshima, Japan
‡‡ Dept. of Civil Eng., Okayama Univ., Okayama, Japan

and few studies have as yet been done on 3-dimensional problems. In particular, there exist a number of problems to be resolved for establishing the simulation system of the crack propagation behavior in 3-dimensional body; that is, the efficient use of the computer system, automatic mesh generator, problems concerning solution accuracy, and so on.

In this investigation the authors propose a numerical simulation system for the crack propagation behavior in arbitrary 3-dimensional body. The system is based on the finite element method and the linear fracture theory is introduced. Moreover, a number of tools are developed and introduced for improving the reliability of the system, i.e. the automatic mesh generation, crack tip area mesh pattern, and so on. Proposed method is applied to actual 3-dimensional problems, and the results are compared with those from the structural experiment. In this paper 2-dimensional analysis is also included with a similar comparison of results with those from structural experiments and 3-dimensional analysis.

2. Structural experiments and results

Results from structural experiments are briefly summarized here, since the main purpose of this investigation is to propose a numerical simulation method for the crack propagation.

2.1. Experiment 1-Crack propagation test for concrete structure

A concrete structure in Fig. 1 is used for the investigation of the crack propagation behavior. A vertical hole with the distance "L" from the front face is drilled into the top surface of the structure, and a wedge with a pair of counter wedges are placed inside the hole as shown in Fig. 2. The top of the wedge is hit by a hammer to generate a pair of cracks on the surface of the vertical hole, and the hitting of the wedge continued until the cracks reach to the front or side faces of the concrete structure. This structural experiment is done for the distance "L" of 30.0, 80.0, and 130.0cm. The aim of this structural experiment is to ascertain the influence

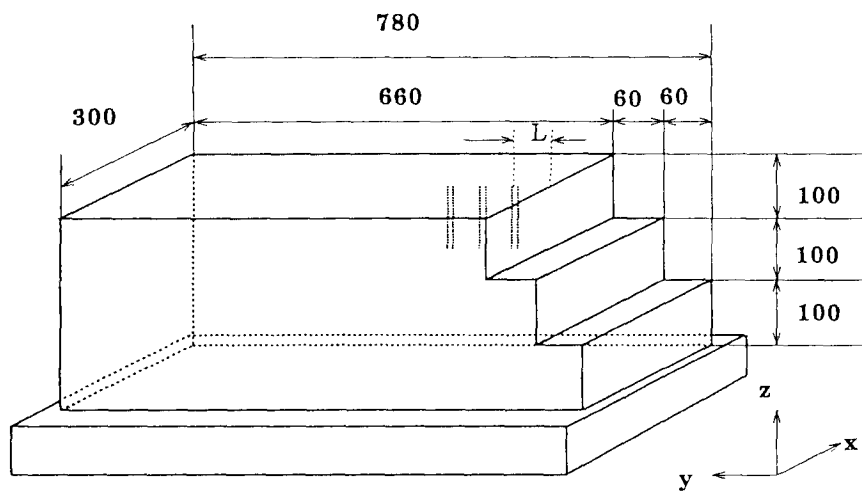

Fig. 1 Concrete Sturucture(cm)

on the distance "L" of the surface crack appearing as a result of the vertical hole.

The results of these experiments are summarized as followings. In the case where $L=30.0$ cm, two cracks on the top surface resulting from the vertical hole change directions to the front face, and they reach there. Fig. 3 illustrates the shape of generated crack. As obvious from this figure, the crack forms on only one surface, and, therefore, two cracks appeared from the hole at the beginning of the experiment join at the bottom of the hole. Henceforth, we divide the cracked surface into three parts (i.e. part A, B and C) as shown in Fig. 3. The position where the crack-tip of the part C appeared on the front face is the corner of the first step of the concrete structure.

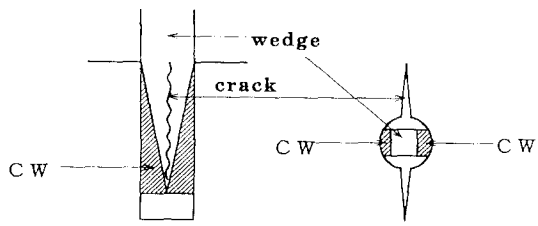

Fig. 2 Loading System

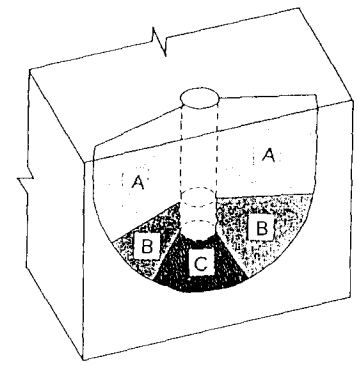

Fig. 3 Shape of Cracked Surface

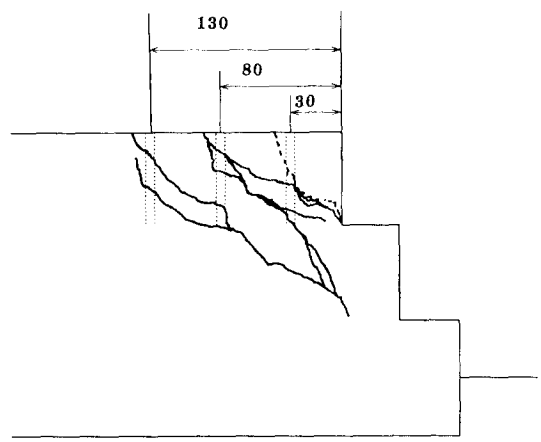

Fig. 4 Crack on Side Face of Structure

In the case where $L=80.0cm$, after both cracks on the top face propagate toward both side surfaces of the structure, they gradually change directions toward the front face, and they reach there. In this case, the part C of the crack appears at the corner of the first step of the structure, and, as a result, the structure is broken as in the first case. But, the volume of the concrete which is removed is larger than that from the first case. Several cracks appear on the side surfaces of the structure, which are illustrated in Fig. 4 by dotted lines.

In the case where $L=130.0cm$, two cracks appeared on the top propagate almost straight toward the side surfaces, and they reach there. Then, they propagate downward as shown in Fig. 4 by thick lines. The experiment is stopped, since their direction goes toward the bottom of the structure. In this experiment a number of cracks appeared on the side surfaces as shown in Fig. 4.

2.2. Experiment 2 – Crack propagation test for acrylic resin specimen

Through Experiment 1 the process of the crack propagation was not clarified, and, a new experiment was planned.

Acrylic resin specimen is newly prepared and used for the experiment in the crack propagation, and the detail of the specimen is shown in Fig. 5. A vertical hole is drilled into the top surface, and a wedge and a pair of counter wedges, which are made of steel, are set into the hole in order to generate a pair of cracks from the hole. The distance "L" of the hole from the front surface is changed in order to ascertain the influence of "L" on the shape of the crack surface. The value "L" is 2.0, 3.0, and $3.5cm$.

In case $L=2.0cm$, the part A of the crack of Fig. 3 appears from the vertical hole and propagates toward the side surfaces. And, it gradually changes direction toward the front face, and it reaches there. After the generation and the propagation of the part A to a certain extent, the portion B and C appear from the bottom part of the vertical hole, and they reach to the front face in a instance. The cracked surface generated through this experiment forms the shape illustrated in Fig. 3.

The behavior of the crack propagation in case $L=3.0cm$ is almost the same as the former case, but the part A of the crack reaches almost to the corner of the front and side surfaces of the specimen. In case $L=3.5cm$, the crack on the top surface of the portiion A reaches to the side surfaces, and the cracks appearing on the side surfaces incline toward the front face and it appears on the front face. This part is connected to the portion B and C, which appear on the front face. These results are summarized in Table 1.

The results of Experiment 1 and 2 are summarized as follows:

(a) The part A of the crack surface starts from the surface of the vertical hole and propagates

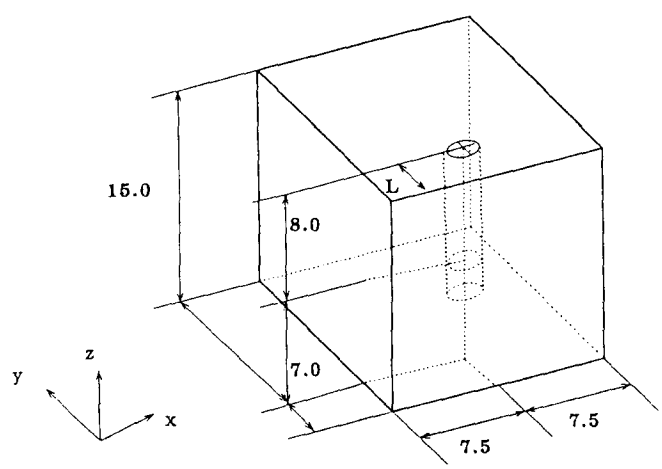

Fig. 5 Acrylic Resin Specimen(cm)

Table 1 Result of Experiment 2

	Distance	Result	
	L (cm)	θ (deg)	ϕ (deg)
Model 1	2.0	25.0	17.0
Model 2	3.0	15.0	20.0
Model 3	3.5	11.0	-

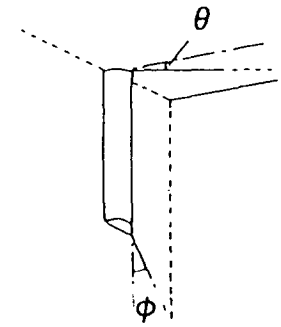

toward the side surfaces of the specimen. It is worth noting that the vertical length of this portion is almost as long as the length of the counter wedge.
(b) This part of crack changes its direction toward the front face as it propagates. The angle of the direction of the propagating crack is influenced by "L", which is the distance between the hole and the front face of the specimen, and the experiments show that the angle tends to become large for small value of "L".
(c) The part C of the crack appears from the bottom of the counter wedge, and it propagates toward the front face.
(d) These experiments can't clarify how the portion B and C of the crack propagate, since the growth of these parts was instantaneous.

3. Crack propagation analysis based on linear fracture theory

It is well-known that the stress distribution near the crack-tip area is singular as shown in Fig. 6, and therefore the most important factors necessary to obtain good computational simulation of the crack propagation behavior in structures are solution accuracy and the numerical stability, since the computational result is governed by the stress distribution near the crack-tip area. Taking these facts into consideration, in this paper we use the displacements instead of stresses as variables, since 1) better numerical stability can be expected and 2) tools necessary for the crack propagation analysis are already proposed using displacements.

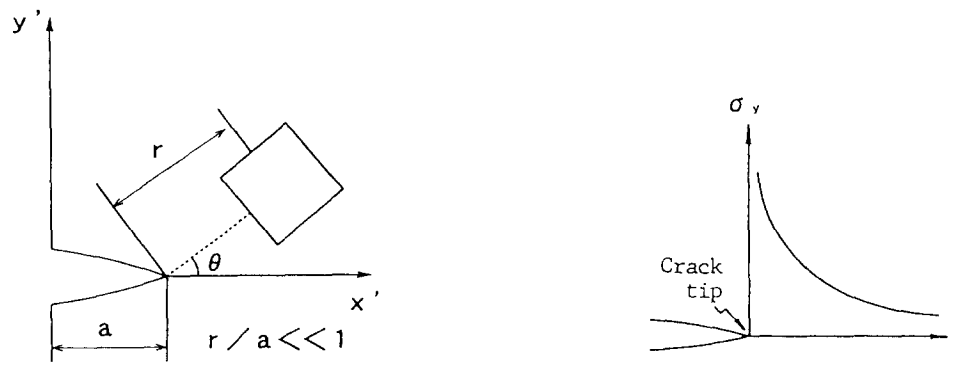

(a) Local Coordinates (b) Stress Distribution

Fig. 6 Singular Stress Distribution near Crack-tip

Among the fracture theories the linear fracture mechanics is adequately investigated. Hence we introduce the theory of the numerical simulation of the crack propagation behavior in 3D structures. But first, we have to clarify 1) the fracture criterion and 2) the direction of the crack propagation. In the linear fracture theory, the stress intensity factor is used instead of the stresses.

3.1. Stress intensity factor

The stress intensity factor is introduced in the linear fracture theory instead of stress and strain, which are used in the theory of elasticity.

The deformation near the crack-tip area is classified into three types as shown in Fig. 7. In case of 2-dimensional problems, only Mode I and Mode II may be considered. Henceforth, we denote the stress intensity factor of these three modes as K_{I}, K_{II} and K_{III}, respectively.

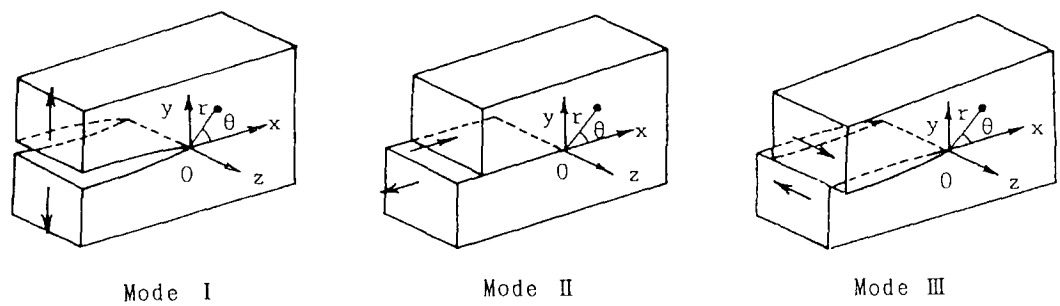

Fig. 7 Three Types of Deformation

These stress intensity factors are analytically derived from the Airy's stress function (Shiraishi, N. et al. 1988), and the stresses and displacements at the crack-tip area are expressed using the following stress intensity factors;

$$\begin{Bmatrix} \sigma_x \\ \sigma_y \\ \tau_{xy} \\ \tau_{yz} \\ \tau_{zx} \end{Bmatrix} = \frac{K_I}{\sqrt{2\pi r}} \begin{Bmatrix} \cos\frac{\theta}{2}\left(1-\sin\frac{\theta}{2}\sin\frac{3}{2}\theta\right) \\ \cos\frac{\theta}{2}\left(1+\sin\frac{\theta}{2}\sin\frac{3}{2}\theta\right) \\ \cos\frac{\theta}{2}\sin\frac{\theta}{2}\cos\frac{3}{2}\theta \\ 0 \\ 0 \end{Bmatrix} + \frac{K_{II}}{\sqrt{2\pi r}} \begin{Bmatrix} -\sin\frac{\theta}{2}\left(2+\cos\frac{\theta}{2}\cos\frac{3}{2}\theta\right) \\ \sin\frac{\theta}{2}\cos\frac{\theta}{2}\cos\frac{3}{2}\theta \\ \cos\frac{\theta}{2}\left(1-\sin\frac{\theta}{2}\sin\frac{3}{2}\theta\right) \\ 0 \\ 0 \end{Bmatrix} + \frac{K_{III}}{\sqrt{2\pi r}} \begin{Bmatrix} 0 \\ 0 \\ 0 \\ \cos\frac{\theta}{2} \\ -\sin\frac{\theta}{2} \end{Bmatrix} \tag{1}$$

$$\begin{Bmatrix} u \\ v \\ w \end{Bmatrix} = \frac{K_I}{G}\sqrt{\frac{r}{2\pi}} \begin{Bmatrix} \cos\frac{\theta}{2}\left(\frac{k-1}{2}+\sin^2\frac{\theta}{2}\right) \\ \sin\frac{\theta}{2}\left(\frac{k+1}{2}-\cos^2\frac{\theta}{2}\right) \\ 0 \end{Bmatrix} + \frac{K_{II}}{G}\sqrt{\frac{r}{2\pi}} \begin{Bmatrix} \sin\frac{\theta}{2}\left(\frac{k+1}{2}+\cos^2\frac{\theta}{2}\right) \\ \cos\frac{\theta}{2}\left(\frac{k-1}{2}-\sin^2\frac{\theta}{2}\right) \\ 0 \end{Bmatrix} + \frac{2K_{III}}{G}\sqrt{\frac{r}{2\pi}} \begin{Bmatrix} 0 \\ 0 \\ \sin\frac{\theta}{2} \end{Bmatrix} \tag{2}$$

where G is the shear modulus, and (r, θ) shows the coordinates of a point as shown in Fig. 6 (a).

Now, we consider the evaluation of these stress intensity factors using the finite element method. As obvious from eq. (2), the displacements are expressed as functions of the root of the distance, r, from the crack-tip. This suggests that the shape function introduced in the finite elements should satisfy this condition. This requirement is satisfied by introducing the singular isoparametric element which is developed by Barsoum (Ingraffea, A.R. 1983).

The singular isoparametric elements are illustrated in Figs. 8 and 9. In 2D problems, two

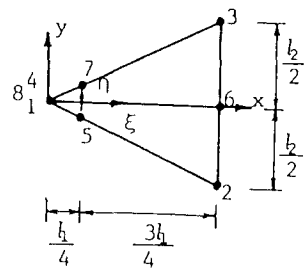

(a) 6-Node Singular Element

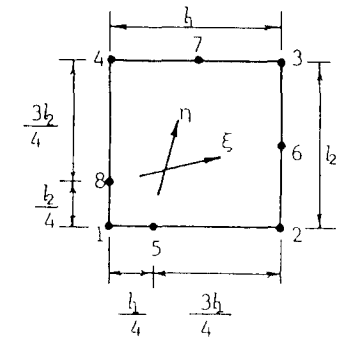

(b) 8-Node Singular Element

Fig. 8 Singular Isoparametric Element for 2D Analysis

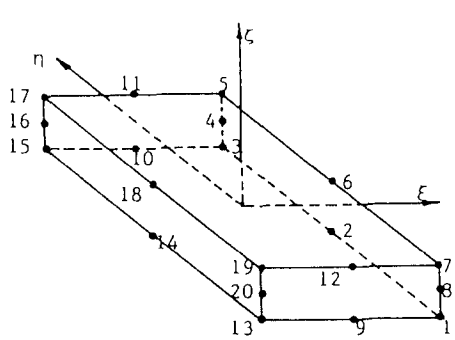

(a) 20-Node Isoparametric Element

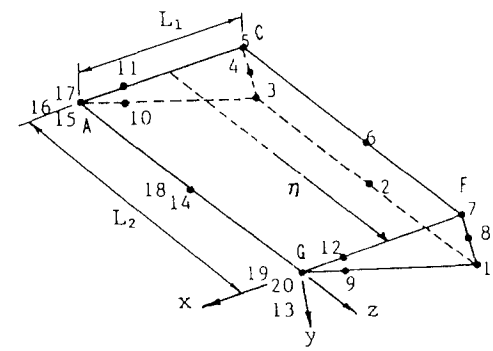

(b) 15-Node Singular Element

Fig. 9 3-Dimensional Element

mid-points on edges adjacent to the crack-tip are moved by 1/4 of the edge lengths toward the crack-tip. (See Fig. 8) In 3D problems, one face of a hexahedral element is first cracked and all mid-points on edges, which are adjacent to the cracked surface, are moved by 1/4 of the edge lengthes toward the cracked surface. In this case, the line which is generated by cracking a surface is used to express a part of the crack-tip. Using these elements, we can express the characteristic of the singular stress distribution at the crack-tip.

In 2D problems, the stress intensity factors are expressed as follows.

$$\begin{aligned} K_I &= \sqrt{\frac{2\pi}{L}}\,\frac{G}{k+1}\,[4(v_B-v_D)+v_E-v_C] \\ K_{II} &= \sqrt{\frac{2\pi}{L}}\,\frac{G}{k+1}\,[4(u_B-u_D)+u_E-u_C] \end{aligned} \tag{3}$$

And, the stress intensity factors for Mode I, II, and III are expressed as follows,

$$\begin{aligned} K_I = \frac{G}{4(k+1)}\sqrt{\frac{2\pi}{L_I}}\,[&2v_B-v_C+2v_E-v_F+v_D \\ &-2v'_B+v'_C-2v'_E+v'_F-v'_D \\ &+\frac{1}{2}\eta(-4v_B+v_C+4v_E-v_F+4v'_B-v'_C-4v'_E+v'_F) \\ &+\frac{1}{2}\eta^2(v_F+v_C-2v_D-v'_F-v'_C+2v'_D)] \end{aligned}$$

$$\begin{aligned} K_{II} = \frac{G}{4(k+1)}\sqrt{\frac{2\pi}{L_I}}\,[&2u_B-u_C+2u_E-u_F+u_D \\ &-2u'_B+u'_C-2u'_E+u'_F-u'_D \\ &+\frac{1}{2}\eta(-4u_B+u_C+4u_E-u_F+4u'_B-u'_C-4u'_E+u'_F) \\ &+\frac{1}{2}\eta^2(u_F+u_C-2u_D-u'_F-u'_C+2u'_D)] \end{aligned} \tag{4}$$

$$\begin{aligned} K_{III} = \frac{G}{4}\sqrt{\frac{2\pi}{L_I}}\,[&2w_B-w_C+2w_E-w_F+w_D \\ &-2w'_B+w'_C-2w'_E+w'_F-w'_D \\ &+\frac{1}{2}\eta(-4w_B+w_C+4w_E-w_F+4w'_B-w'_C-4w'_E+w'_F) \\ &+\frac{1}{2}\eta^2(w_F+w_C-2w_D-w'_F-w'_C+2w'_D)] \end{aligned}$$

where all notations in eqs. (3) and (4) are shown in Fig. 10. Note that "η" has a value between -1 and $+1$, and for each value above equations can express the displacement at any position between the edges AC and GF.

3.2. Fracture criterion

The purpose of this investigation is to numerically simulate the propagation process of a crack which appears in 3D elastic body. A great number of structural experiments have been done in order to clarify the appearance and the growth of cracks, and one of the fracture criteria is that the fracture occurs at the site of the maximum tensile stress. Using this criterion

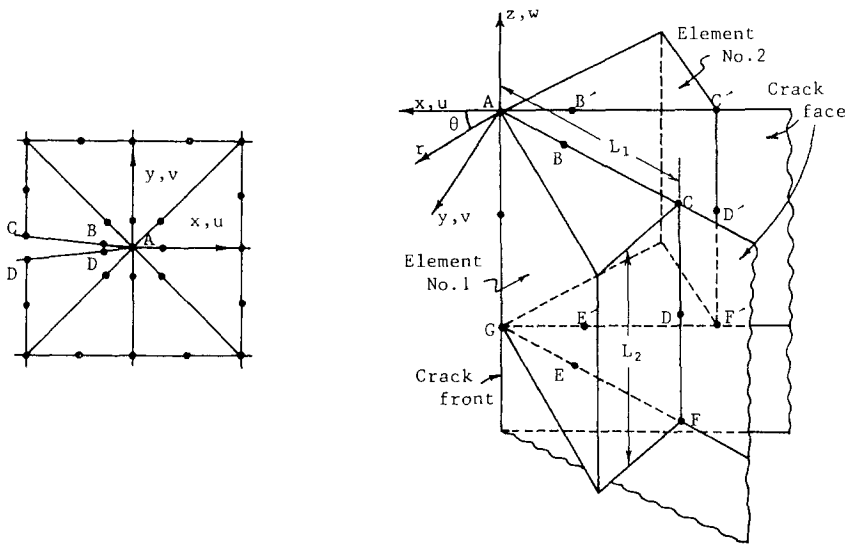

Fig. 10 Nodes at Crack-tip Area

and also taking the linear theory into the consideration, the crack, at first, occurs at the place where the maximum tensile stress appears in the body, and it successively grows to the element which has the maximum tensile stress.

3.3. Direction of crack propagation

In analyzing the 2-dimensional crack propagation behavior, the direction of the propagating crack and the length of propagation must be determined at every stage of the analysis. Using these two values, new position of the crack-tip is determined in the domain, and a new model is generated for the successive analysis.

Here, we assume that the growth of the crack is appropriately decided by the user. On the determination of its direction, we have following theories:

Maximum Stress Criterion (Erdogan, F. & Sih, G.C. 1963)

Minimum Strain Energy Density Criterion (Sih, G.C. 1972)

Criterion of Symmetry (Gol'dstein, R.V. & Salganik, R.L. 1974)

Maximum Energy Release Rate Criterion (Wu, C.H. 1978)

The first criterion is that the crack grows in the direction normal to the direction of the maximum tensile stress, which occurs among elements at crack-tip. The second criterion shows that the crack grows in the direction where the strain energy density becomes minimum. Thus, these two criteria are available for determining the direction of the crack growth using the model which is used in this present analysis.

On the other hand, the third and fourth criteria require setting imaginary crack growth for determining the direction. The third criterion suggests that new crack growth occurs toward the direction where the stress intensity factor, K_{II}, becomes zero. And the last criterion indicates that the crack propagates so that its growth can release the maximum energy.

As is clear from the above, the latter two criteria require additional computation compar-

ing to the former two. We therefore introduce the maximum stress criterion in our method.

In the 3-dimensional problem, we have to consider three modes as shown in Fig. 7. The first criterion is easily introduced in this case, and, therefore, the maximum stress criterion is used for our investigation. We assume that the crack grows from the tip by one element-size for each analysis.

3.4. Mesh generation

As far as the finite element method is used for the analysis, the model must be renewed according to the growth of the crack. It is worth noting that the crack-tip area must be carefully modelled, since the stress distribution is singular there. Now, the authors consider the mesh generation for the finite element analysis.

First we consider on the 2-dimensional problem. We introduce the singular isoparametric element at the crack-tip. As mentioned already, the singular element can theoratically express the characteristics of the deformation at the crack. Then, we can expect good results, if the size of the element is appropriately decided. For this purpose, we propose a mesh pattern as shown in Fig. 11, which is always introduced at the crack-tip. The singular isoparametric element is introduced for 8 triangular elements located at the crack-tip, and other triangular and quadrilateral elements are normal isoparametric elements (Taniguchi, T. et al. 1987). The user may decide only the diameter of the circular envelope of the mesh pattern, and mesh sizes of all elements in Fig. 11 are automatically decided. This mesh pattern is always set at the crack-tip, which changes position in accordance with the crack propagation.

The domain of the analysis is first divided into triangular elements using the Delaunay triangulation, which one of the authors of this paper already proposed in Taniguchi, T. et al. 1991a. That is, nodes on all boundaries and also on the crack line are first introduced, and the Delaunay triangulation is applied for these nodes in order to define the domain and also to divide it into triangles. At the same time, the crack line is generated using edges of generated triangles. Successively, nodes are automatically generated in the domain using the quadtree method, and the Delaunay triangulation is applied again so that the domain which is already coarsely triangulated is divided into finer trianglar meshes. After this triangulatioin, the mesh

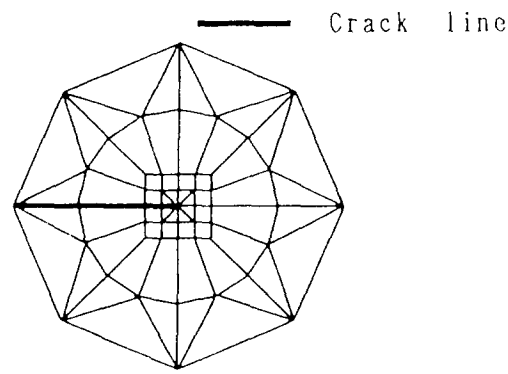

Fig. 11 Meshes at Crack-tip

pattern mentioned above is introduced at the crack-tip, and the smoothing of generated meshes is achieved using the Laplacian method, which moves each node to the center of gravity of the area of all triangles that enclose the node. Refer to Taniguchi, T. et al. 1991a,b in the details of the mesh generation.

Now, we describe the mesh generation for the 3D analysis of the specimen shown in Fig. 5. In order to obtain good numerical results fine meshes must be arranged near the crack-tip, and, finer meshes must be prepared especially in the portion where the crack changes direction. On the other hand, the modelling of 3D body necessarily requires numerous nodes, and, therefore, how to set nodes in the domain, how to divide the domain into elements and the characteristics of elements to be introduced decide the accuracy of the analysis. The result of the structural experiment summarized in previous section gives an important suggestion for the numerical modelling. According to the experiments, it is expected that the stress distribution of the part B and C of the crack surface is relatively complex compared to the part A. Then, we divide these domains using finer meshes, and the residual using coarse meshes.

From the viewpoint of the computational mechanics, it is preferable to model whole domain using only the hexahedral elements. But, we have to abandon the modelling of the domain using only the hexahedral elements, since 1) there exist no available mesh generator which can divide arbitrary 3D domain into hexahedral elements, 2) the finite element model must be renewed in accordance with the growth of the crack surface, and 3) the shape of the crack surface is a curved one, and, therefore, the subdivision of the domain into hexahedral elements necessarily generates distorted elements. Then, we introduce other type of elements as the triangular prisum and tetrahedral elements with hexahedral elements.

Taking the symmetricity of the structure into consideration, we can treat only half of the specimen as shown in Fig. 12. The vertical hole is replaced by a slit as shown in the figure, since the hole is expanded in the y direction using a wedge and counter wedges. This slit is used as a initial crack for the crack propagation analysis. Then, we obtain the finite element model as shown in Fig. 13. The domain is divided using three types of finite elements, i.e. hexahedra, triangular prisms, and tetrahedra. Considering the growth of the crack, triangular prism and tetrahedral elements are placed in the subdomain where the crack surface has geo-

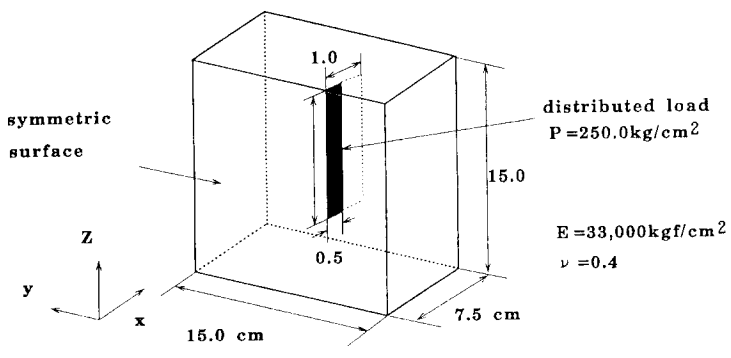

Fig. 12 Structural for 3D Analysis

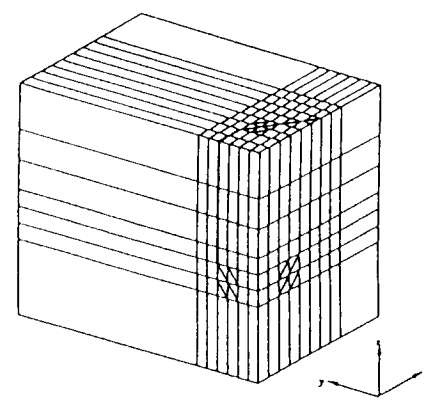

Fig. 13 Finite Element Model

metrical complexity. That is, triangular prisms are used for expressing the part A and C of the crack, and tetrahedral elements are used at the crossing domain of triangular prisms which includes the part B of Fig. 3. Above procedure for generating a finite element model can also generate the surface which is used as the initial crack surface. Additional operation is required to prepare the isnitial crack surface. That is, new node is generated for each node on the crack surface as to have the same position. This operation is done for all nodes on the surface except nodes located at the crack–tip, and another side of the crack surface is generated using these new nodes.

In accordance with the crack growth we have to modify the finite element model, and this modification is achieved as follows; At each stage of the analysis the direction of new crack growth is determined. Then, nodes to be prepared for expressing the crack surface are moved to the position where the crack grows, and the new nodes are prepared for expressing additional crack surface. It should be noted that at every analysis the elements located at the crack–tip are used for generating new crack surface. Therefore, at the stage of generating the initial finite element model, fine elements must be prepared in the domain where the crack propagates.

4. Numerical simulation of 2D crack propagation

In this section we numerically simulate the crack propagation behavior in a certain plane of the concrete structure shown in Fig. 1. As is clear from the structure in Fig. 1 and the loading method in Fig. 2, there exists a symmetric plane which is parallel to the yz plane and paths through the center of the vertical hole. Through this 2–dimensional analysis we can clarify the crack propagation behavior of the portion C in Fig. 3. Another 2–dimensional analysis can be achieved in the xy plane which cuts the vertical hole horizontally, and this numerical analysis can clarify the crack propagation of the portion A of Fig. 3.

For both analyses we have to set the assumption of the plane strain, and, henceforth, we call these two models Model 1 and Model 2, respectively. At the beginning of the crack propagation analysis, first we have to set the initial crack. In Model 1 we set a slit as long as the length of the counter wedge, since the structural experiment shows that the crack of the part C starts from the bottom of the counter wedge. In Model 2, we may treat only a half of the domain for the analysis because of the symmetricity of the structure. The initial crack for this model is a slit of the length of the radius of the vertical hole, and it is set at the position of the hole. Uniform load is applied to all nodes located on the initial crack surface. The material constants used for the analysis are summarized in Table 2.

Table 2 Material Constants

Material	Young's Modulus (kgf/cm^2)	Poisson's Ratio
Concrete	300,000	0.20
Soil	3,000	0.45

The flowchart of the crack propagation analysis is shown in Fig. 14. Throughout the analysis, a large sparse set of linear algebraic equations must be solved as many times as the num-

ber of the crack propagations, and we introduce the skyline solver for this purpose (Bathe, K.J. & Wilson, E.L. 1976). And, for the saving of necessary memories and also for the saving of the execution time, we introduce the Gibbs–Poole–Stockmeyer algorithm for the node reordering method (Gibbs, N.E. et al. 1976).

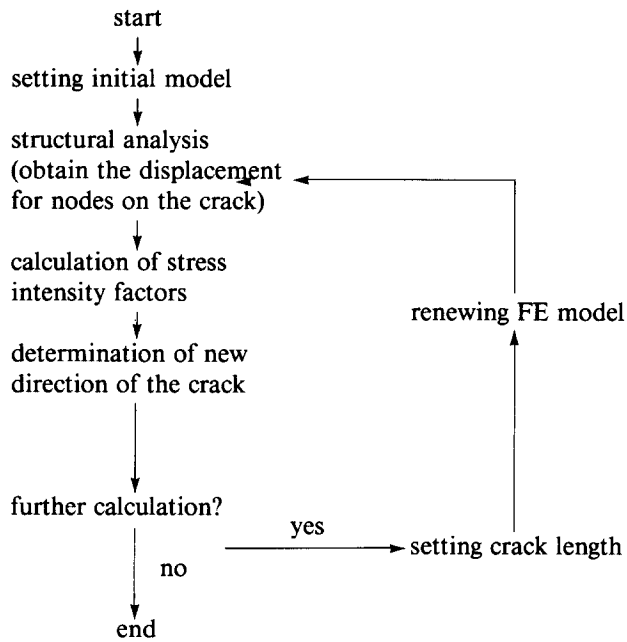

Fig. 14 Flowchart of Analysis

4.1. Numerical result of model 1

The computation is done for three cases of initial crack, which located 30, 80 and 130cm from the front face of the structure, and the results are shown in Figs. 15, 16 and 17, respectively. Thick lines in these figures show the paths of the crack propagation from the beginning to the final state of the computation. In the case of the distance of $L=30cm$, the crack goes almost straight to the corner of the first step of the concrete structure. In case $L=80cm$, the crack first goes downward and successively changes direction toward the corner of the first step. In the last case $L=130cm$, the analysis shows that the crack reaches to the corner of the second step of the structure, but we may actually judge that the crack propagates toward the corner of the third step of the structure, since the change of the angle toward the corner of the second step is too abrupt. Actual cracks observed in the structural experiment may become the evidence of our judgement. (See the cracks shown in Fig. 4) Summarizing these results, we can conclude that the numerical simulation shows good coincidence with the experimental results.

4.2. Numerical result of model 2

As in the above numerical tests, three models with $L=30$, 80 and 130cm are prepared

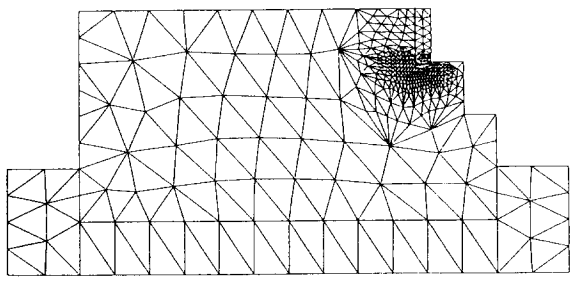

Fig. 15 Model 1(L=30cm)

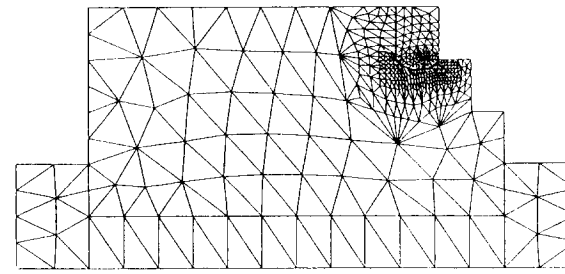

Fig. 16 Model 1(L=80cm)

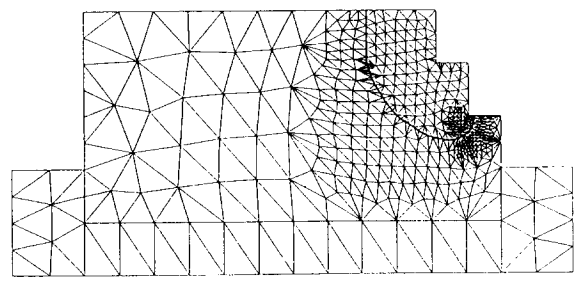

Fig. 17 Model 1(L=130cm)

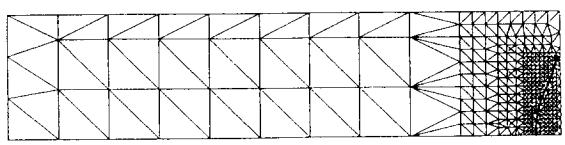

Fig. 18 Model 2(L=30cm)

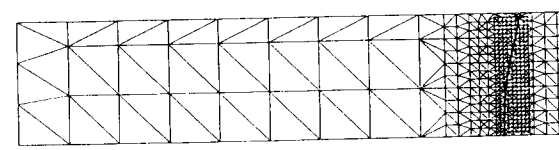

Fig. 19 Model 2(L=80cm)

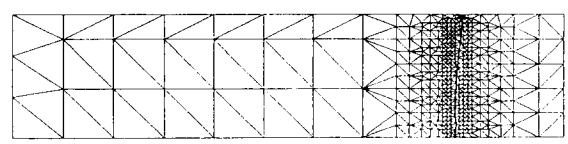

Fig. 20 Model 2(L=130cm)

and used for the numerical experiments. The paths obtained from the numerical simulation are shown in Figs. 18, 19 and 20, respectively. In case $L=30cm$, the crack growing from the initial one changes direction toward the front face of the structure, and it reaches there. Comparing this result with the experiment, the behavior by the numerical simulation shows good coincidence with the structural experiment. In cases $L=80$ and $130cm$, the crack propagates toward the side face of the structure and it reaches there, but in the structural experiments the crack in $L=80cm$ reaches the front face. On the other hand, the numerical result of $L=130$ cm coincides with the experimental one.

Summarizing all results of the numerical experiments using the 2-dimensional models, we obtain following conclusions.

(1) The crack propagation behavior in the concrete structure can be numerically simulated using the linear fracture theory, though there exists slight difference between the structural and numerical ones.

(2) For clarifying the crack propagation behavior in the part of A and C, the 2-dimensional analysis is available with the assumption of the plane strain.

(3) The difference between the numerical and structural experiments may be caused by following reasons; a) the loading method may differ from the actual experiment, b) the fracture theory which is introduced here is linear but the actual one may be nonlinear, and c) in the calculation only one crack is treated, but in the actual experiments there occur a number of cracks.

(4) The behavior of the crack in the part B can't be treated as 2-dimensional problem, and the behavior can be clarified only by 3-dimensional analysis.

5. Numerical simulation of 3D crack propagation

Using the finite element model shown in Fig. 13, the behavior of the crack propagation in the acrylite resin specimen is investigated. The model consists of hexahedral, triangular prism with tetrahedral finite elements, all of which are isoparametric. All nodes on the initial crack surface are subject to a uniformly distributed load of $250kgf/cm^2$. The initial crack is placed at the distance of 2.0, 3.0 and $3.5cm$ from the front face of the specimen.

We assume that the crack propagates in the element which has the maximum tensile stress due to load, and direction is determined using the maximum tensile stress criterion. Then, the meshes near the crack-tip area are moved so as to coincide with the direction where the crack propagates, and this finite element model is used for the successive analyses. Young's modulas and Poisson's ratio used for the experiments are $33{,}000kg/cm$ and 0.4, respectively. The procedure in the crack propagation analysis is just the same as the one shown in Fig. 14. The initial finite element model has 2488 nodes.

Now, we summarize the result of the numerical simulation. Fig. 21 shows the final displacement states of the crack surface for three cases, and Fig. 22 shows the process of the crack propagation for $L=2.0cm$. The darker zone in Fig. 22 shows the crack surface newly generated at the step. It should be noted that these two figures show only a part of the specimen where the crack is located, and the residal part is removed. The results shown in Fig. 21 are very similar to the cracks actually observed in the structural experiments. And, the process of the crack propagation illustrated in Fig. 22 clarifies that the crack begins to grow from the part A and successively from the part B, and finally the part C. Fig. 23 shows the stress distribution of elements in the planes which are parallel to the xy plane. This figure clarifies the

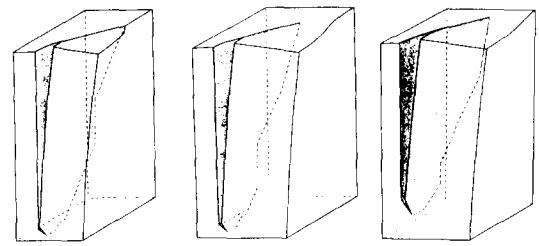

Fig. 21 Crack Surfaces

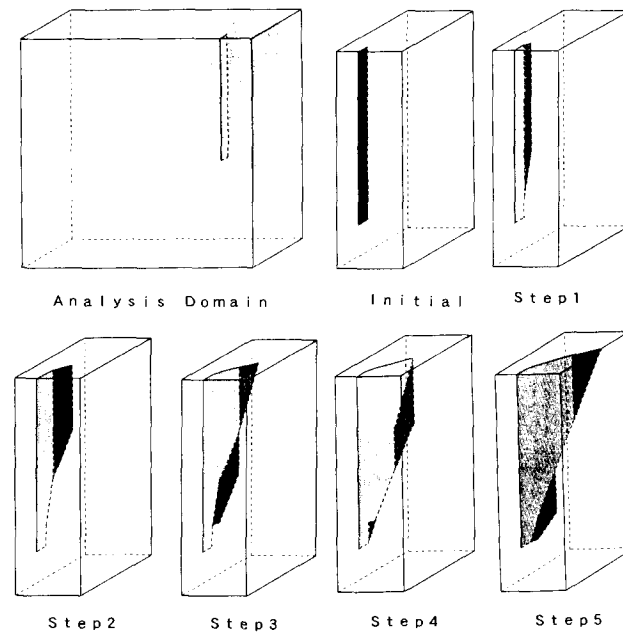

Fig. 22 Propagation of Crack(L=2.0cm)

fact that in accordance with the crack propagation the maximum tensile stress always appears in the elements located at the crack-tip.

The crack propagations on the symmetric and top surfaces of the model are shown in Fig. 24(a) and (b), respectively. The results show that the crack has the stronger tendency going toward the front face for shorter distance between the hole and the front face, and this result coincides with the experimental one. The paths of cracks in Fig. 24(b) show good coincidence with the cracks obtained by the experiments, but the results in Fig. 24(a) give smaller angles compared to the experimental one. This difference may be caused by the coarse meshes in the part B and C, which located at the bottom of the model.

6. Concluding remarks

In this investigation the crack propagation behavior occurring in 3D body is numerically simulated using the displacement-type finite element method based on the linear fracture the-

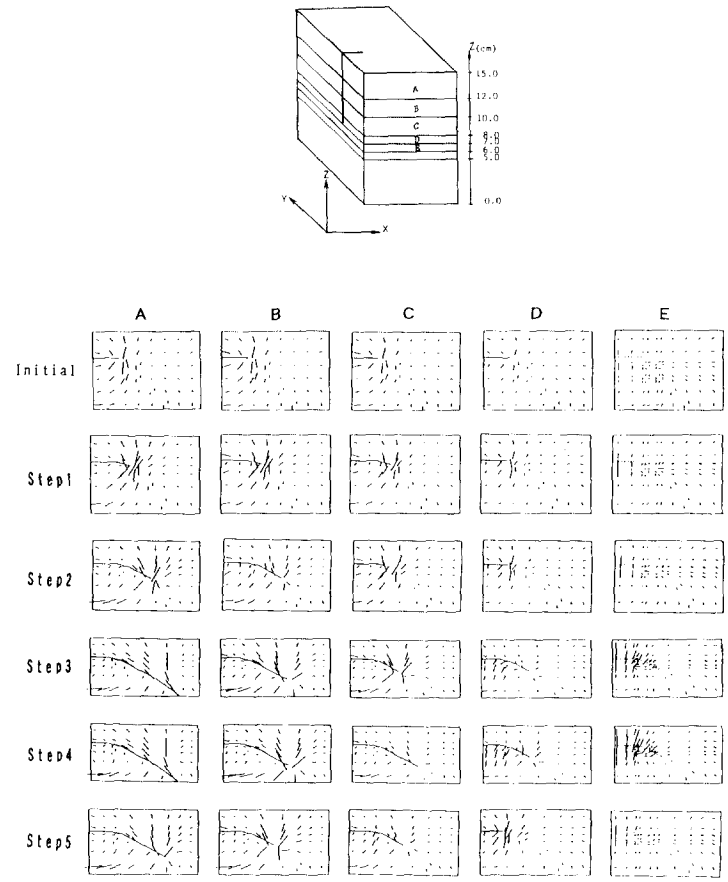

Fig. 23 Stress Distribution due to Crack Propagation

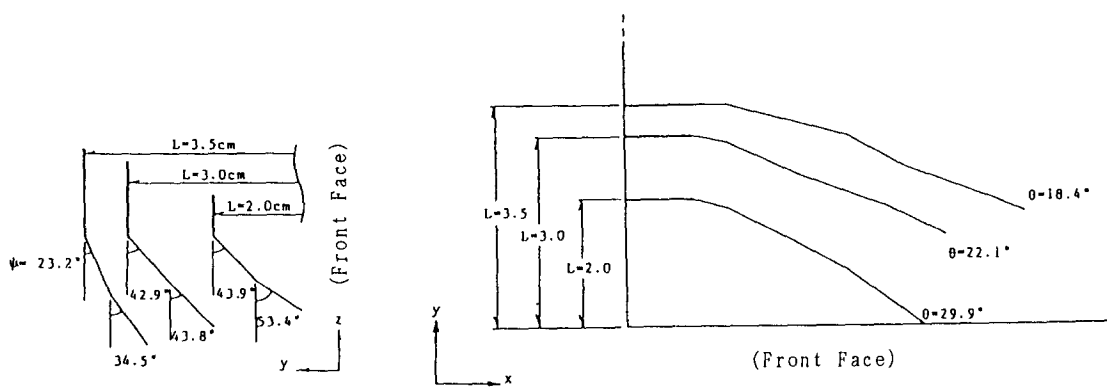

(a) On Symmetric Surface (b) On Top Surface

Fig. 24 Crack Propagation

ory. The analysis is made in terms of both 2-and 3-dimensions and the computational results are compared with the crack propagation obtained by the structural experiments. The results of the 2D analysis show good coincidence with the experimental one, and the results of the 3D analysis show also good coincidence except for the behavior of the crack appearing at the bottom part of the specimen. Summarizing these results, we may conclude that the behavior of the crack in 3D body can be numerically simulated using the linear fracture theory. Further improvement in the computational result may be expected when finer meshes can be prepared in the modelling.

For the 3D numerical simulation of the crack propagation an effective automatic mesh generator is strongly recommended. At present we can expect only the mesh generator based on the Delaunay triangulation which can prepare only tetrahedral elements. From the computational point of view, the finite element model using only hexahedral elements is preferable.

References

Bathe, K.J. & Wilson, E.L. (1976), *Numerical methods in finite element analysis,* Prentice-Hall.

Erdogan, F. & Sih, G.C. (1963), "On the crack extension in plates under plane loading and transverse shear", *Trans, ASME,* December, 519-527.

Gibbs, N.E., Poole, W.G. & Stockmeyer, P.K. (1976), "Algorithm for reducing the bandwidth and profile of sparse matrix?, *SIAM J. of Numerical Analysis,* **13**, 236-263.

Gol'dstein, R.V. & Salganik, R.L. (1974), "Brittle fracture of solids with arbitrary cracks", *Int. J. of Fracture,* **10**, 507-523.

Ingraffea, A.R. (1983), "Numerical modelling of fracture propagation", *Rock Fracture Mechanics* (ed. Rothmaith, H.P., Springer, Berlin, 151-208.

Miyaji, A. & Takahashi, K. (1985), "A study on the mechanics of the rock cutting using wedge", Technical Report of Japan Development and Construction Co., Ltd., 8, 65-72. (In Japanese)

Shiraishi, N., Ohnishi, Y. & Taniguchi, T. (1988), *Continuum mechanics,* Morikita Publishing Co., Tokyo, 95-127. (In Japanese)

Sih, G.C. (1972), "Introductory chapter, A special theory of crack propagation", *Mechanics of fracture,* **1**, 21-45.

Taniguchi, T. & Ohta, C. (1991a), "Application of the Delaunay triangulation for arbitrary 2D domain closed by a set of straight lines", *Proc. JSCE,* **432** (I-16), 69-78. (In Japanese)

Taniguchi, T. & Ohta, C. (1991b), "Delaunay-based grid generation for 3D body with complex boundary geometry", 3rd Int. Conf. on *Numerical Grid Generation in Computational Fluid Mechanics and Related Field* (eds. Arcilla, A.S. et al.). 533-543.

Taniguchi, T., Sanada, K., Matsumoto, H. & Moriwaki, S. (1987), "Some remarks on finite element modelling on crack-tip area", Memoirs of the School of Engineering, Okayama University, **21** (2), 31-46.

Wu, C.H. (1978), "Maximum-energy-release rate criterion applied to a tension-compression specimen with crack", *Journal of Elasticity,* **8**, 235-257.